Anal. Calcd for $C_6H_8N_2O_3$: C, 46.15; H, 5.16; N, 17.94. Found: C, 46.18; H, 5.06; N, 17.81.

The melting point of this material was undepressed on admixture with 1,3-dimethyl-5-hydroxyuracil (VI) (mp 201–201.5°) obtained by published methods.[13] The two compounds were completely identical with regard to ir, nmr spectra, and R_f values on tlc.

1,3-Dimethyl-5-acetoxyuracil (VII). A mixture of 1,3-dimethyluracil (I) (300 mg), acetic anhydride (2 ml), and dry pyridine (5 ml) was kept at 50° for 12 hr and then evaporated to dryness *in vacuo*. The residue was dissolved in methylene chloride. The solution after filtration through a silica gel column (10 × 50 mm) and removal of the solvent gave colorless crystals. Recrystallization from a mixture of methylene chloride–ether gave 257 mg of colorless prisms, mp 150–151.5°.

Anal. Calcd for $C_6H_{10}NO_4$: C, 48.48; H, 5.09; N, 14.14. Found: C, 48.03; H, 4.60; N, 14.52.

Reduction of 1,3-Dimethyl-5-hydroxy-5,6-dihydrouracil (VIII) with Sodium Borohydride. To a stirred solution of 1.0 g of 1,3-dimethyl-5-hydroxy-5,6-dihydrouracil (VIII) in 100 ml of 50% aqueous methanol was added 250 mg of sodium borohydride. After 30 min another 250 mg of sodium borohydride was added and the mechanical stirring continued for 2 hr. The resulting solution was passed through an Amberlite IRC-50 (H^+ form) column in order to remove the sodium ion. The filtrate was lyophilized and the residue dissolved in *methanol* and evaporated *in vacuo*. This procedure was repeated three or four times until all the boric acid had been removed. The reduction product was chromatographed on a column of silica gel (20 × 280 mm), the column was eluted with a mixture of chloroform and methanol (8:2), and fractions of 6 ml were collected.

Fractions 15–30 (600 mg) were collected and purified twice on silica gel and finally by preparative thin layer chromatography to give the glycol XII as a homogeneous amorphous powder (R_f 0.51; solvent A), mol wt, 160 (mass spectrum). The following were obtained: ir (liquid film) (cm^{-1}): 3448 (NH), 1618 (ureido); nmr (CD_3OD) (ppm): 2.92 (>NCH_3), 2.98 (>NCH_3), 3.0–3.8 (m) (>NCH_2CH–), 4.67 (m) (2>$CHOH$).

Acetate. The acetate was prepared with acetic anhydride in pyridine. Recrystallization from ether gave colorless prisms, mp 111.5–112°.

Anal. Calcd for $C_8H_{14}N_2O_4$: C, 47.52; H, 6.98; N, 13.86; mol wt, 202. Found: C, 47.55; H, 6.91; N, 13.78; mol wt, 202 (mass spectrum).

The following data were obtained: ir (Nujol) (cm^{-1}): 3311 (–OH), 1742 (acetyl), 1645 (sh), 1629 (ureido); nmr ($CDCl_3$) (ppm): 2.07 (CH_3CO–), 2.92 (>NCH_3), 2.99 (>NCH_3), 3.00–3.98 (m) (>NCH_2CH–), 4.76 (q, J_1 = 2.5 cps, J_2 = 3 cps), 4.87 (d, J = 2.5 cps), 5.35 (broad) (OH).

Fractions 12–14 (400 mg) were purified by preparative tlc. The band corresponding to R_f 0.55 (solvent B) was separated, eluted, and acetylated with acetic anhydride in pyridine. The hydroscopic acetate formed colorless prisms: ir (liquid film) (cm^{-1}): 1742 (acetyl), 1650 (ureido), 1230 (acetyl), 1080 and 1742 (ν_{C-O}); nmr ($CDCl_3$) (ppm): 2.08 (acetyl), 2.95 (>NCH_3), 3.08 (>NCH_3), 3.47 (–OCH_3), 3.50 (m) (>NCH_2CH–), 4.41 (q, J_1 = 1.7 cps, J_2 = 2.8 cps) (>CHO), 4.96 (q, J_1 = 2.8 cps, J_2 = 5 cps) (>CHO).

Studies on Models for Tetrahydrofolic Acid. I. The Condensation of Formaldehyde with Tetrahydroquinoxaline Analogs

Stephen J. Benkovic,[1] Patricia A. Benkovic, and David R. Comfort

Contribution from the Department of Chemistry, The Pennsylvania State University, University Park, Pennsylvania 16802. *Received April 7, 1969*

Abstract: To investigate the mechanisms of tetrahydrofolic acid catalyzed one carbon unit transfers, we have synthesized several tetrahydroquinoxaline analogs. A kinetic investigation of the condensation with formaldehyde of one of these models reveals the intermediacy of the iminium cation as a steady-state species and the importance of general catalysis in formation of the imidazolidine ring, the latter a model for 5,10-methylenetetrahydrofolic acid. The relevance of these results to the mechanism of one carbon unit transfers and the importance of certain structural and electronic features in the actual cofactor are discussed.

The intermediacy of N^5,N^{10}-methylenetetrahydrofolic acid in the transfer of one carbon unit at the oxidation level of formaldehyde in various enzymic reac-

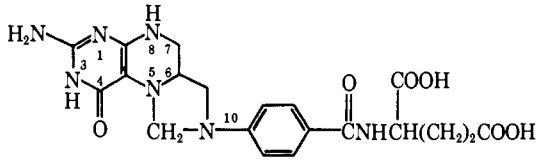

tions including the interconversion of glycine and serine and the formation of 5-hydroxymethyldeoxycytidylic acid and deoxythymidylic acid illustrates its importance in biosynthesis.[2] The molecular arena comprised of the 5-nitrogen of the reduced pyrazine ring and the 10-nitrogen of the *p*-aminobenzamide residue also provide many challenging mechanistic questions concerned with the actual pathway of the carbon transfer, challenges further complicated by the instability of the actual cofactor.

We have approached this problem by designing model analogs predicated on the desirability of simplifying experimental problems through removal of several "nonessential" dissociable groups subject, however, to the following considerations.

It is apparent from the extensive work of Baker, *et al.*,[3] on analogs of tetrahydrofolic acid designed to act as nonclassical antimetabolites against dihydrofolate reductase and the structure–activity analysis of their inhibition by the method of Hansch[4] that a major function of the pyrimidine ring of the pteridine moiety is the binding of the cofactor to the enzyme. This is

(1) Alfred Sloan Fellow, 1968–1970.

(2) M. Friedkin, *Ann. Rev. Biochem.*, 32, 185 (1963), and references therein.

(3) B. R. Baker, "Design of Active-Site-Directed Irreversible Enzyme Inhibitors," John Wiley & Sons, Inc., New York, N. Y., 1967.

(4) E. Miller and C. Hansch, *J. Pharm. Sci.*, 56, 92 (1967).

probably the primary function of the glutamate residue. A second function of the pyrimidine ring is revealed by the recent measurements of Kallen and Jencks of the dissociation constants of tetrahydrofolic acid.[5] The important 5-nitrogen and 10-nitrogen sites have pK_a' values of 4.82 and −1.25, respectively. The unusually low pK_a' of the 10-nitrogen presumably arises from the electrostatic interactions with the protonated 5-nitrogen and 1-nitrogen with the higher pK_a' of the 5-nitrogen being a result of the relatively greater electron density at the 5 position of a pyrimidine ring.[6] Thus elimination of the 4-hydroxy-2-aminopyrimidine residue on the basis of its contribution to the instability of the tetrahydropteridine,[7] multiple dissociations, and importance in enzyme–substrate binding must be compensated for in terms of its effect on the pK_a' of the designed models. A final consideration is the requirement of an unsymmetrical molecule in order to study migrations of carbon units between the 5-nitrogen and 10-nitrogen sites. In this paper we wish to discuss the results of our investigation of the synthesis of tetrahydroquinoxaline analogs **1** and **2** and the condensation of formaldehyde with **1**.

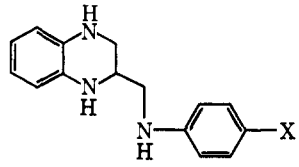

1, X = $COOC_2H_5$
2, X = CH_3

Results

The synthesis of the tetrahydroquinoxaline derivatives involved the condensations of quinoxaline-2-aldehyde with the *para*-substituted anilines to yield the known anils followed by their reduction to the tetrahydroquinoxaline compounds. Reduction methods employing catalytic hydrogenation (platinum oxide–glacial acetic acid or Raney nickel–tetrahydrofuran) yielded a mixture of reduced products that were difficult to resolve. Separation by column chromatography (silica gel) of the reaction products from the platinum oxide–glacial acetic acid hydrogenation of the *p*-carboethoxyanil yielded a major component identified as 2-methyl-1,2,3,-4-tetrahydroquinoxaline arising from cleavage at the imine bond. Proposed reduction of the *p*-carboethoxyanil imine double bond with sodium borohydride in diglyme gave fortuitously complete reduction to the tetrahydroquinoxaline derivative (48% yield). The anil formed by condensation of toluidine with quinoxaline-2-aldehyde likewise was reduced to the tetrahydro derivative with sodium borohydride in diglyme or lithium aluminum hydride in diethyl ether.

The presence of the tetrahydro structure was deduced from the following evidence. The mass spectrum fragmentation pattern of **2** showed a molecular ion peak *m/e* 253 (theoretical 253) and two intense peaks at *m/e* 133 and 120, corresponding to an anticipated cleavage between C-2 of the tetrahydroquinoxaline ring and the exocyclic carbon[8] leading to the resonance-stabilized ions, either $C_8H_9N_2^+$ or $C_8H_{10}N^+$. The nmr spectrum in $CDCl_3$ of **2** shows a doublet at δ 7.0 (2 H, aromatic), a complex multiplet centered at 6.6 (6 H, aromatic), a singlet at 3.7 (3 H–N), a complex multiplet centered at 3.2 (5 HC–N), and a singlet at 2.2 (3 H, CH_3) relative to TMS. The ultraviolet spectrum exhibits three absorption bands ($\lambda_{max}^{ethanol}$) at 310 mμ (ε 5100), 251 (15,000) and 218 (28,600) characteristic of tetrahydroquinoxaline structures.[9,10] Compound **1** ionizes to a mass spectrum fragmentation pattern with parent ion *m/e* 310 (theoretical *m/e* 311) and two intense peaks at *m/e* 133 and 178, again resulting from scission between the tetrahydroquinoxaline ring carbon and methylene of the side chain. The nmr spectrum of **1** in acetone shows a doublet at δ 7.8 (2 H, aromatic), an unsymmetrical triplet centered at 6.6 (6 H, aromatic), a quartet at 4.3 (2 H, CO_2CH_2–), a broad absorption at *ca.* 3.0–4.0 (3 H–N), a complex multiplet centered at 3.3 (5 HC–N), and a triplet at 1.3 (3 H, $CO_2CH_2CH_3$). The ultraviolet spectrum reveals two absorption bands ($\lambda_{max}^{ethanol}$) at 308 mμ (ε 25,400) and 221 (31,100). The ultraviolet spectra of both **1** and **2** are pH dependent with **1** exhibiting a third $\lambda_{max}^{H_2O}$ at 235 mμ at pH <2.0.

The addition of formaldehyde in aqueous dioxane (kinetic runs) or in ethanol to either **1** or **2** (molar ratio 1:1) forms an adduct to which we have assigned the five-membered imidazolidine ring structure. The infrared spectrum of **3** reveals diminished absorption at

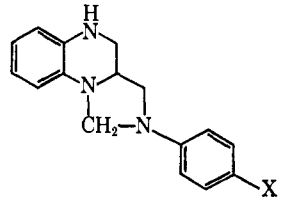

3, X = $COOC_2H_5$
4, X = CH_3

3350 cm^{-1} from loss of N–H. The mass spectrum of **3** has a parent ion at *m/e* 323 (theoretical *m/e* 323) suggesting the monomer. The ultraviolet absorption spectrum of **3** reveals λ_{max} (50% v/v dioxane–water) at 310 mμ (ε 32,900) and 221 mμ. The absence of a blue shift and/or a decrease in the intensity of the 310-mμ band is consistent with five-membered rather than six-membered ring formation since the latter structure (**5**), although relatively angle strain free, constrains the lone pair of electrons at the 4-nitrogen to be approximately orthogonal to the π electrons of the adjacent phenyl ring. The spectroscopic effects of steric hindrance in conjugated systems and, in particular, aniline resonance generally are manifested by a strong decrease in the in-

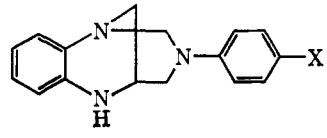

5

tensity of the long-wavelength bands (>250 mμ) as in

(5) R. G. Kallen and W. P. Jencks, *J. Biol. Chem.*, **241**, 5845 (1966).
(6) A. R. Katritzky and J. M. Lagowski, "Heterocyclic Chemistry," John Wiley & Sons, Inc., New York, N. Y., 1960.
(7) E. C. Taylor and W. R. Sherman, *J. Am. Chem. Soc.*, **81**, 2464 (1959).
(8) K. Biemann, "Mass Spectrometry: Organic Chemical Applications," McGraw-Hill Book Co., Inc., New York, N. Y., 1962.
(9) M. Munk and H. P. Schultz, *J. Am. Chem. Soc.*, 74, 3434 (1952).
(10) G. Henseke and R. Jacobi, *Ann.*, **684**, 153 (1965).

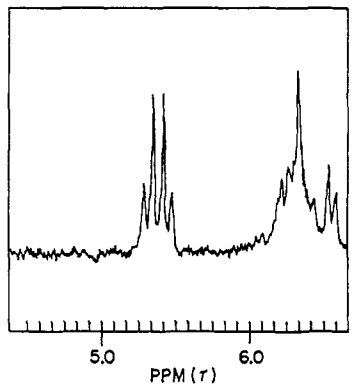

Figure 1. The nmr spectrum of **4** in $CDCl_3$.

the series dimethylaniline, *o*-methyldimethylaniline, and *o,o*-dimethyldimethylaniline where ϵ decreases in the order 2300 > 1200 > 0 at λ_{max} 296 mμ.[11,12] The loss of intensity must be accounted for almost entirely by the steric inhibition of aniline resonance.[12] To corroborate this reasoning we have synthesized the corresponding unequivocal tetrahydroquinoline adduct **6**[13] and this compound, like **3**, has an absorption band at 310 mμ, the λ_{max} unchanged relative to the parent diamine **7** but increased in intensity by *ca.* 20%. Monoprotonation of **1** which occurs on the tetrahydroquinoxaline moiety and to a first approximation may be equated with loss of conjugation results in a shift of $\lambda_{max}^{H_2O}$ from 308 to 302 mμ and a 6% decrease in the intensity of the band. Like **3** the ultraviolet spectrum of **4** shows an increase in intensity at 310 mμ and in addition at 254 mμ.

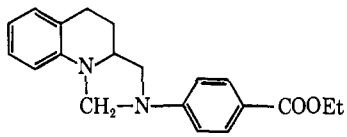

6

The assignment of structures **3** and **4** to the formaldehyde adducts is confirmed by the nmr spectra of these compounds. The nmr spectra in $CDCl_3$ of **4** shows a partially resolved doublet at δ 7.0 (2 H, aromatic), a multiplet at 6.6 (6 H, aromatic), a singlet at 2.2 (3 H, CH_3), a complex multiplet 3.0–3.9 (5 HC–N), and a new resonance band centered at 4.63 (>NCH_2N<) (Figure 1). The latter is an AB quartet with J_{ab} = 4 cps and δ_{ab} 10 cps. The nmr spectrum in dioxane of **3**, although not integrated due to problems of solubility, displays the AB quartet of >NCH_2N< centered at δ 4.74 with J_{ab} = 5 cps and δ_{ab} 9 cps. For comparison the nmr spectrum of **6** has the characteristic AB quartet of >NCH_2N< at δ 4.52 with J_{ab} = 4 cps and δ_{ab} 8 cps. This characteristic geminal coupling constant may be contrasted with a J_{ab} = 9 cps of N,N′-dimethylhexahydropyrimidine[14] and J_{ab} = 10 cps of trimethylhexahydro-1,3,5-triazine[15] for the >NCH_2N< protons (below the coalescence temperature for ring interconversion) of these six-membered ring compounds. Although the spectrum of a N,N′-diphenyl analog is not presently available, it is anticipated that the difference between J_{ab} for the two isomers (five- *vs.* six-membered ring) will be magnified by phenyl substitution.[16]

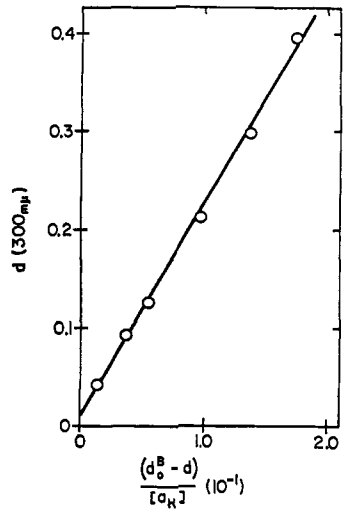

Figure 2. Plot of optical density (d) at 300 mμ for **1** as a function of the ratio of dication concentration to hydrogen ion activity where d_0^B is the optical density of pure monocation (25°).

The pH dependency of the ultraviolet absorbance of **1**, **7**, and **3** was utilized to determine their pK_a' values. Plots of OD at pH-sensitive wavelengths as a function of the relative proportions of base to conjugate acid (Figure 2) for the various substrates provide the data of Table I.

Table I

Substrate	λ, mμ	Solvent	pK_a' (25°)
1	300[a]	H_2O	−0.33 ± 0.02[b]
	225	H_2O	4.35 ± 0.1
	230	50% v/v dioxane–H_2O, μ = 0.2	3.78 ± 0.03
7	300[c]	H_2O	−1.10 ± 0.05[b]
	250	50% v/v dioxane–H_2O, μ = 0.2	2.58 ± 0.03
3	225	50% v/v dioxane–H_2O, μ = 0.2	2.88 ± 0.07[d]

[a] Band undergoes hypsochromic shift upon successive protonation: λ_{max} 308 → 302 (pK_a' = 4.35); λ_{max} 303 → 293 (pK_a' = −0.33). [b] Relative to H_0. [c] Band undergoes hypsochromic shift upon protonation: λ_{max} 306 → 300 (pK_a' ≈4.0); λ_{max} 300, however, shows no shift upon second protonation. [d] No higher pK_a' detected up to pH 6.

The pseudo-first-order rate (k_{obsd}) for formation of the formaldehyde adduct from substrate **1** was determined spectrophotometrically from the time-dependent increase in absorbance at 310 mμ (solvent 50% v/v dioxane–H_2O, μ = 0.2, 25°). In the case of **1** k_{obsd} changes from first order to zero order in formaldehyde concentration as the latter is varied from 0 to 8.83 × 10^{-4}–1.67 × 10^{-3} *M* over the pH range 3.5–9.1. Reciprocal plots of k_{obsd} *vs.* $[CH_2(OH)_2]$[17] yield as the intercept at

(11) W. R. Remington, *J. Am. Chem. Soc.*, 67, 1838 (1945).
(12) H. B. Klevens and J. R. Platt, *ibid.*, 71, 1714 (1949).
(13) S. J. Benkovic and R. Chrzanowski, unpublished results.
(14) F. G. Riddell, *J. Chem. Soc., B*, 560 (1967).
(15) J. M. Lehn, F. G. Riddell, B. J. Price, and I. O. Sutherland, *ibid., B*, 387 (1967).
(16) M. Barfield and D. M. Grant, *J. Am. Chem. Soc.*, 85, 1899 (1963).
(17) Formaldehyde is nearly completely hydrated in aqueous solution, but its rate of dehydration to free formaldehyde would not be rate controlling under the conditions of this study: P. Le Hénaff, *Compt. Rend.*, 256, 1752 (1963).

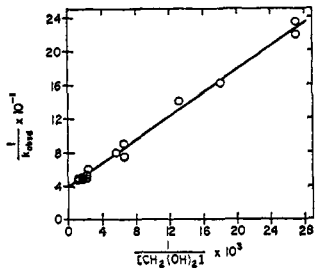

Figure 3. Plot of the reciprocal of k_{obsd} for **1** *vs.* the reciprocal of formaldehyde concentration at 0.08 *M* acetate, pH 5.43 (μ = 0.2, 50% v/v dioxane–water, 25°).

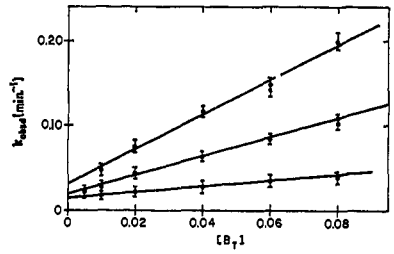

Figure 4. Graph of k_{obsd} for **1** as a function of total acetate buffer concentration at pH 5.43, 6.06, and 6.64, slope decreasing with increasing pH. Conditions: 50% v/v dioxane–water, 25°, μ = 0.2, $[CH_2(OH)_2]$ at 6.60 × 10^{-4} *M*.

the ordinate the reciprocal of the maximum pseudo-first-order rate constant at saturating formaldehyde concentrations (subject to buffer effects) and as the intercept at the abscissa the negative of the equilibrium constant (K_1') for formation of the intermediate. The latter intercept which is apparently independent of buffer effects was measured at pH 3.87, 4.54, 5.43, and 6.64 through a series of experiments similar to those illustrated in Figure 3.[18] The values of K_1' are dependent on the mole fraction of **1** in the free base form which when corrected gives K_1 = 5.5 × 10^3 ± 1.1 M^{-1}.[19] No inhibition of k_{obsd} as evidenced by a positive deviation near the origin on a double reciprocal plot was observed. Consequently experiments designed to study k_{obsd} as a function of pH for substrate **1** were conducted at saturating $[CH_2(OH)_2]$ of 6.60 × 10^{-4}–1.33 × 10^{-3} *M* where k_{obsd} is experimentally independent of formaldehyde concentration and the kinetics are pseudo first order [**1** ≅ 2.0 × 10^{-5} *M*].[20] The rapid formation of a reaction intermediate inferred from the above also is detected upon initiation of the kinetic run by the "immediate" decrease (10–15%) in the absorbance at 310 mμ. A rapid scan (pH 7.7) disclosed the spectrum of the intermediate to have λ_{max} similar to **1**. This behavior results in a lag phase at early times in the plots of log (OD_∞ − OD_t) against time employed to calculate k_{obsd}.

(18) Strictly speaking the abscissa intercept is subject to buffer effects because the magnitude and nature of the buffer catalysis should vary with the change in the kinetic order of $[CH_2(OH)_2]$. The values of K_1' were checked by extrapolating k_{obsd} at several different $[CH_2(OH)_2]$ to zero buffer concentration at the above pH values and the same results (Figure 3) were obtained. Evidently the buffer effects are self-cancelling.

(19) Calculated from $K_1' = K_1(K_a/(K_a + H^+))$ where K_a' = 1.74 × 10^{-4}.

(20) Control experiments in which $[CH_2(OH)_2]$ was varied at low total buffer concentration (0.02 *M*) at pH 4.50, 5.39, and 6.64 established that k_{obsd} remained independent of formaldehyde concentration.

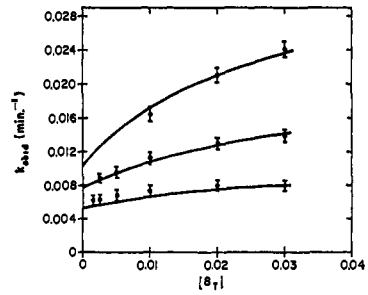

Figure 5. Graph of k_{obsd} for **1** as a function of total phosphate buffer concentration at pH 7.10, 7.45, and 7.73, slope decreasing with increasing pH. Solid line from eq 2.

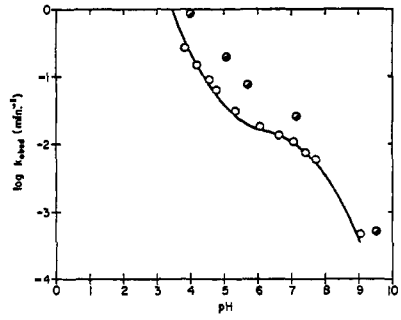

Figure 6. Plot of the logarithm of k_{obsd} for **1** extrapolated to zero buffer concentration against pH, μ = 0.2, 25°, 50% v/v dioxane–water. The points (◒) are in 20% v/v dioxane–water. Solid line from eq 1.

The rate constants for the condensation of formaldehyde with **1** are dependent upon the nature and concentration of the buffer species. The pH–rate profile for k_{obsd} was established by extrapolating the latter values to zero buffer concentration as illustrated for acetate (Figure 4) and phosphate buffers (Figure 5). The extrapolated rate constants as a function of pH are depicted in Figure 6. The unusual features of this profile—not anticipated for simple acid-catalyzed dehydration of a carbinolamine intermediate—can be satisfactorily simulated by the following expression for k_{obsd} as a function of pH

$$k_{obsd} = \frac{[A(H^+) + B](H^+)}{(H^+) + C} \qquad (1)$$

where A = 2.30 × 10^3, B = 1.50 × 10^{-2}, and C = 3.56 × 10^{-8}.[21] That this behavior is not the result of solvent composition or specific salt effects is demonstrated by the data obtained in 20% v/v dioxane–water (Figure 6) and the fact that changes in μ do not alter the magnitude of k_{obsd}.

Inspection of Figures 4 and 5 reveals that the sensitivity of the condensation reaction to buffer catalysis markedly depends on the latter's chemical identity. Whereas catalysis at constant pH is apparently directly proportional to total buffer concentration for formate (not shown) and acetate buffers, a changing order is observed with phosphate. The rate expression for the be-

(21) Reiterative calculations. The parametric value of A has been slightly altered from that previously reported by increasing the accuracy of the extrapolation to zero buffer concentration through additional kinetic runs. The involvement of a dissociable group at low pH does not now provide an adequate description of the kinetics (S. J. Benkovic, P. A. Benkovic, and D. R. Comfort, *J. Am. Chem. Soc.*, **91**, 1860 (1969).

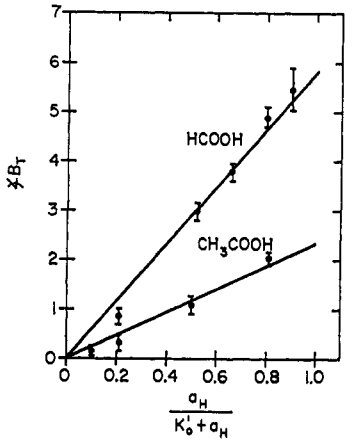

Figure 7. Graph of the pH-dependent rate constant for buffer catalysis as a function of the mole fraction of buffer in the acid form for formate and acetate.

havior of k_{obsd} in the presence of buffer is given by

$$k_{obsd} = \frac{(A(H^+) + B + D[HA])(H^+)}{C + (1 + E[A])(H^+)} \quad (2)$$

where the parametric values D and E vary with the nature of the buffer species. In the case of formate and acetate $(H^+) \gg C$ and $E[A]$, in particular at those pH values $\ll pK_a'$ of the buffer. This condition is best satisfied at pH 3.87 and pH 5.43 for formate and acetate, respectively, where the rate law then simplifies to

$$k_{obsd} = D[HA] \quad (3)$$

omitting the intercept term due to lyate species. A graph of the slopes of the plots for formate and for acetate as a function of the mole fraction of buffer in the acidic form is presented in Figure 7. Examination of Figure 7 verifies that the buffers are acting as general acid catalysts with no detectable contribution arising from the basic species. The interpretation of the data is weighted to favor those kinetic runs at pH $< pK_a'$ because calculations with eq 2 indicate that the term $E[A]$ may be significant yet remain unrecognized as $E[A] \approx 1$ owing to a limited variation in buffer concentration. Consequently at pH values where the given buffer was predominantly in the basic form, the measurements of k_{obsd} were conducted at minimal buffer concentrations and overlapped with a second buffer of differing chemical composition mainly present as the acidic species. The values of D are listed in Table II.

Table II. Calculated Values for the Parametric Values Employed in Equations 1-3

Parameters	Species	Numerical[a]
A	Lyate	$2.30 \times 10^3\ M^{-1}\ min^{-1}$
B	Lyate	$1.50 \times 10^{-2}\ min^{-1}$
C	Lyate	$3.55 \times 10^{-8}\ M$
D	Formate	$5.80\ M^{-1}\ min^{-1}$ [b]
D	Acetate	$2.30\ M^{-1}\ min^{-1}$ [b]
D	Phosphate	$1.97\ M^{-1}\ min^{-1}$ [b]
E	Phosphate	$175\ M^{-1}\ min^{-1}$ [b]

[a] Values apply to experiments conducted at $\mu = 0.2$, 25°, 50% v/v dioxane-H_2O under conditions where kinetics are zero order in $[CH_2(OH)_2]$. [b] Estimated error ±10%.

Catalysis by phosphate buffers follows eq 3 at pH 7.10 being directly proportional to buffer concentration. At pH 7.45–7.73 the rate initially increases linearly with low buffer concentration but tends to become zero order in buffer at higher buffer concentrations. Employing reiterative calculations, we are able to accommodate satisfactorily the experimental data with the values of D and E tabulated in Table II.

Discussion

The synthesis of **1** and **2** *via* the sodium borohydride reduction provides a simple efficient means of entry into this class of compounds. Earlier attempts to reduce only the exocyclic azomethine double bond with catalytic hydrogenation disclosed that the quinoxaline ring was reduced at least as readily.[22] The stereospecific reduction of 2,3-dimethylquinoxaline by lithium aluminum hydride to the *cis*-2,3-dimethyltetrahydroquinoxaline moreover established precedence for strong metal hydride–quinoxaline complexation.[23] The fact that reactions employing sodium borohydride and designed to yield tetrahydroquinoxaline derivatives are generally *only* effective with quinoxaline quaternary salts[24] argues that the successful use of this metal hydride for reduction of **1** and **2** is most likely the result of a favorable geometry for solvent-dependent five- or six-membered ring complexation owing to the imino side chain. It is noteworthy that a related reaction involving the imine bond of ethyl *p*-(2-pyrazal)aminobenzoate with excess sodium borohydride in methanol yields the product of only exocyclic azomethine reduction, ethyl *p*-(2-pyrazinylmethyl)aminobenzoate.[25] Possible protonation or hydrogen bonding by methanol to anionic species generated during the borohydride reduction may prevent productive complexation leading to tetrahydro product.[26] The sodium borohydride–diglyme system, however, does not effect reduction in the quinoline series owing to the latter's unfavorable oxidation–reduction potential.[13]

A total of two dissociable groups are found either spectrophotometrically or potentiometrically and their assignment in order of increasing acidity is as follows. Monoprotonation of **1**, established by potentiometric titration, in water or in 50% v/v dioxane–water is associated with a hypsochromic shift of the long-wavelength absorption maximum from 308 to 302 mμ accompanied by a slight decrease in absorption, and a hyperchromic effect at 225 mμ. Similar shifts are detected upon monoprotonation of *o*-phenylenediamine (289–280 mμ)[27] and *trans*-2,3-dimethyltetrahydroquinoxaline (300–295 mμ)[23] which are associated with a 5–10% decrease in absorption. The spectral features (λ_{max}, ϵ) obtained upon monoprotonation of **1** approach **3**, consistent with but not identical with the results obtained with *o*-phenylenediamine whose spectrum is converted upon monoprotonation to one indistinguishable

(22) C. L. Leese and H. N. Rydon, *J. Chem. Soc.*, 308 (1955); A. Kjaer, *Acta. Chem. Scand.*, 2, 456 (1948); R. M. Acheson, *J. Chem. Soc.*, 4731 (1956).
(23) R. C. DeSelms and H. S. Mosher, *J. Am. Chem. Soc.*, 82, 3762 (1960).
(24) R. F. Smith, W. J. Rebel, and T. N. Beach, *J. Org. Chem.*, 24, 205 (1959).
(25) M. P. Mertes and N. R. Patel, *J. Med. Chem.*, 9, 868 (1966).
(26) Reduction of the quinoxaline anils by sodium borohydride in methanol does not yield the tetrahydro derivative: S. J. Benkovic and D. R. Comfort, unpublished results.
(27) P. K. Gallagher, *J. Phys. Chem.*, 67, 807 (1963).

from aniline. Potentiometric titration of tetrahydroquinoxaline in aqueous solution has established a thermodynamic monoprotonation pK_a of 4.84.[28] Our values for **1**, pK_a' of 4.35 in water and 3.78 in 50% v/v dioxane–water, are, therefore, assigned to one or both nitrogens of the tetrahydroquinoxaline ring. The greater acidity is attributed to an inductive or field effect exerted by the exocyclic nitrogen and falls within a calculated $\Delta pK_a'$ (0.90) obtained by comparing the pK_a' values for N-methylaniline and for monoprotonation of N,N′-diphenylethylenediamine.[29,30] Spectrophotometric titration of the tetrahydroquinoline analog (**7**) reveals that monoprotonation is associated with a more acidic pK_a' of 2.58 (50% v/v dioxane–H_2O). Since a large $\Delta pK_a'$ exists between the two amino groups within this molecule owing to unequal electronic effects (estimated pK_a of 2.6 for N-methyl-*p*-carboethoxyaniline and 4.7 for tetrahydroquinoline[30] neglecting the mutual intramolecular perturbation), it is reasonable to assume that the above pK_a' represents mainly protonation of the ring nitrogen. We can then interpret the pK_a' of 4.35 for **1** as signifying that protonation of **1** is largely on the 4-nitrogen of the tetrahydroquinoxaline ring but owing to the proximity and similar basicity of the 1-nitrogen, viewed prior to protonation, the pK_a' values are macroscopic, representing an average of the protonic equilibrium between these two sites. The next question to be answered is the site and extent of additional protonation.

Potentiometric titration of **1** does not reveal a second pK_a' within the reliable range of the electrode and spectrophotometric changes only again become apparent in the H_0 region. Protonation of the cationic quinoline analog (**7**) occurs on a group of $pK_a' = -1.10$ producing a decrease in absorption at 300 mμ, whereas the acidification of **1** causes an *ca.* eightfold decrease in absorption associated with a hypsochromic shift from 303 to 293 mμ. Tetrahydroquinoxaline also undergoes a shift in the position of λ_{max} from 304 to 290 mμ in strong acid.[23] Undoubtedly the site of protonation in **7** is the exocyclic amino group with its low pK_a' being the result of electron withdrawal by the *p*-carboethoxy substituent and the close proximity of a positive charge. The fact that this pK_a' is *lower* than **1** must mean that only one cationic site is present on **1** and that the spectra changes are associated with addition of a second proton. The acid strengthening of a positive charge in **7** is *ca.* 3.7 pH units referred to N-methyl-*p*-carboethoxyaniline. This exceeds the upper limit of the range of 1.5–3.1 pH units derived from literature comparisons by Kallen and Jencks[5] for the acid-strengthening effect of one positive charge separated by two carbon atoms from an amino group and most likely reflects a reduced number of conformational states. The presence of two positive charges as encountered in 2,2′-diaminodiethylamine or in tetrahydrofolic acid (protonation of 1-nitrogen and 5-nitrogen) depresses the most acidic pK_a' by 5–7 pH units. We conclude therefore that the pK_a' of −0.33 represents monoprotonation of the monocation of **1** and is again a macroscopic pK_a' measuring the protonic equilibria between a ring and exocyclic nitrogen, since the respective pK_a' values of the monocation of tetrahydroquinoxaline and N-methyl-*p*-carboethoxyaniline are 2.1 and 2.6 and thus overlap. For comparison the pK_a' of the 5-nitrogen and 10-nitrogen of tetrahydrofolic acid in water ($\mu = 1.0$, 25°) are 4.8 and −1.25, respectively.[5] Finally the lower pK_a' associated with monoprotonation of **3** serves as further supporting evidence for the imidazolidine structure since in the case of **5** the disruption of resonance should act to augment basicity.

An unusual aspect of the kinetics obtained with **1** is the rapid preequilibrium formation of carbinolamine in 10^{-4} *M* formaldehyde solutions at pH values as low as 3.8. From the experiments of DeLuis[31] and Skell[32] and Kallen and Jencks[33] steric requirements of the amine primarily control the magnitude of the equilibrium constant for the addition of formaldehyde to the amine, which is nearly insensitive to the latter's pK_a. The equilibrium constant for formation of carbinolamine (K_1) from **1** corrected by a factor of 2 for the reduced activity of water in the mixed solvent is $2.2 \pm 0.5 \times 10^3$ M^{-1} and is characteristic of secondary cyclic amines (proline, pyrrolidine, piperidine) whose equilibria values range from 76 to 1600 M^{-1}. The formaldehyde affinity for secondary acyclic amines is much smaller, in the range 2–40 M^{-1}. The possibility that the initial intermediate is **5** which then rearranges is discounted on the following grounds: (1) the ultraviolet spectrum closely resembles **1** and (2) rearrangement of **5** to **3** must proceed through an immonium cation or carbinolamine involving the exocyclic nitrogen either of which are less stable than the corresponding intermediates for direct conversion of **1** → **3** with the result that the immediate pathway is favored for a process under kinetic control.

Our results, therefore, are in accord with kinetically productive carbinolamine formation involving a tetrahydroquinoxaline ring nitrogen. We are unable to exclude kinetically unproductive carbinolamine formation at the 4-nitrogen which would affect the value of K_1 but can rule out the formation of an unreactive dihydroxymethyl adduct involving the exocyclic amino group because of the lack of rate inhibition at higher formaldehyde concentrations (Figure 3). This evidence supports the above contention that K_1 for carbinolamine formation at the 10-nitrogen is small. Moreover by employing average values for the formaldehyde affinity of cyclic and acyclic secondary amines we calculate that a reaction pathway involving carbinolamine formation at the exocyclic nitrogen should account for only a maximum of 5% of product formation. The parametric values listed in Table II, therefore, should represent the kinetic constants for conversion of carbinolamine (**8**) to the imidazolidine product.

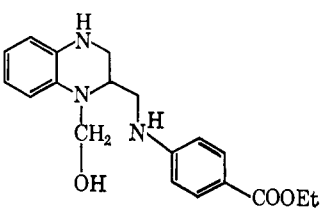

8

(28) J. C. Cavagnol and G. Wilson, Jr., *J. Am. Chem. Soc.*, 72, 3752 (1950).
(29) L. Jaenicke and E. Brode, *Ann.*, **624**, 120 (1959).
(30) A. Albert and E. P. Serjeant, "Ionization Constants of Acids and Bases," Methuen and Co., London, 1962.
(31) J. DeLuis, Thesis, The Pennsylvania State University, 1964.
(32) P. A. Krapcho and H. Suhr, unpublished results; P. S. Skell, personal communication.
(33) R. G. Kallen and W. P. Jencks, *J. Biol. Chem.*, **241**, 5864 (1966).

The unique features of the pH–rate profile must arise from the conversion of carbinolamine to product. Although numerous investigations[34] have demonstrated that dehydration of **8** proceeds almost entirely through hydronium ion catalysis (Brønsted α = 0.7–0.9), this profile does not follow first-order acid-catalyzed dehydration. The kinetic results may only be explained in terms of a steady-state species, logically the iminium cation **9**, whose partitioning is subject to pH control.[35] Two mechanisms are proposed which yield the requisite expression for k_{obsd} (Scheme I or Scheme II)

Scheme I

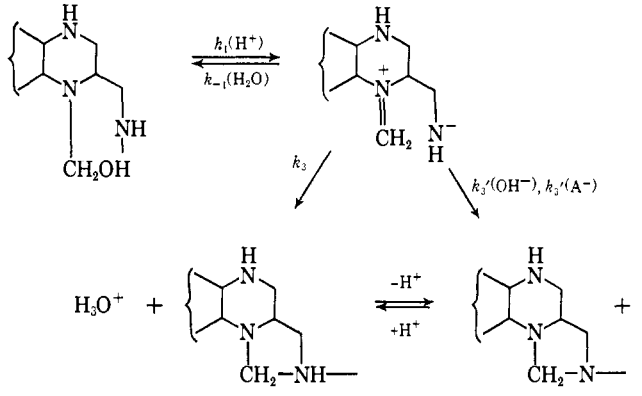

Scheme II

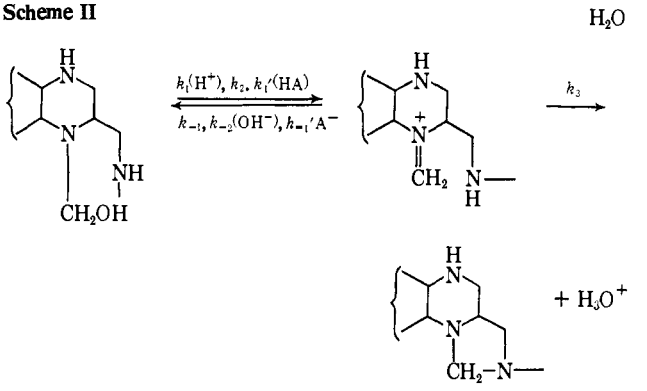

The latter neglects $k_3'(OH^-)$ but includes an additional uncatalyzed dehydration term, k_2, and the associated $k_{-2}(OH^-)$ term. In the absence of buffer catalysis Schemes I and II reduce to eq 1; with appreciable buffer catalysis both schemes furnish eq 2. The parametric values are identified with their respective rate constants in Table III. The above expressions are limiting cases of a general scheme which involves catalysis in both partitioning steps of the iminium cation intermediate. Solution of the latter generates kinetic terms which are second order in buffer but were not observed kinetically. Moreover the limiting cases adequately describe the observed kinetics and, as discussed below, additional evidence implies that one is a unique solution.

In the case of Scheme I the three main features of the pH–rate profile are described as follows: (1) pH 3.5–4.5; $A(H^+) > B$ and $(H^+) \gg C$, with $k_{obsd} = k_3k_1(H^+)/(k_{-1} + k_3)$; (2) pH 5.5–7.0; $B > A(H^+)$ and $(H^+) > C$, with $k_{obsd} = k_3'K_{wD}k_1/(k_{-1} + k_3)$; and (3) pH 8.0–9.0; $B \gg A(H^+)$ and $C > (H^+)$ with $k_{obsd} = k_1(H^+)$. Scheme I, therefore, may be analyzed in terms of rate-determining transitions from water to base-catalyzed ring closure and ultimately rate-determining acid-catalyzed dehydration with increasing pH. In the case of Scheme II the profile results from changes in the rate-determining step from acid-catalyzed to spontaneous dehydration of carbinolamine and ultimately ring closure with increasing pH. The above pH–rate profile, therefore, is similar to other kinetic situations encountered in the addition reactions of nitrogen bases with carbonyl compounds which feature a rate decrease owing to a change in a rate-determining step.[36] Since in the present case this cannot be due to a dissociation of substrate (the pK_a values of carbinolamines are 2–3 pH units less than the parent amines),[33] the rate decrease must reflect a change in the rate steps leading to and from the reaction intermediate.

Table III

Scheme I	Scheme II
$A = \frac{k_3k_1}{(k_{-1} + k_3)}$	$A = \frac{k_3k_1}{(k_{-1} + k_3)}$
$B = \frac{k_3'K_{wD}{}^a k_1}{(k_{-1} + k_3)}$	$B = \frac{k_3k_2}{(k_{-1} + k_3)}$
$C = \frac{k_3'K_{wD}}{(k_{-1} + k_3)}$	$C = \frac{k_{-2}K_{wD}}{(k_{-1} + k_3)}$
$D = \frac{k_3''k_1K_a'{}^b}{(k_{-1} + k_3)}$	$D = \frac{k_3k_1''}{(k_{-1} + k_3)}$
$E = \frac{k_3''}{(k_{-1} + k_3)}$	$E = \frac{k_{-1}''}{(k_{-1} + k_3)}$

[a] K_{wD} is defined as the autoprotolysis constant of H_2O in 50% dioxane–H_2O, 25°, equal to 1.80×10^{-16} (H. S. Harned and B. B. Owen, "The Physical Chemistry of Electrolytic Solutions," Reinhold Publishing Corp., New York, N. Y., 1950). [b] K_a' is defined as the dissociation of the conjugate acid of the buffer species in 50% v/v dioxane–H_2O, μ = 0.2, 25°.

Additional supporting evidence for a change in the rate-determining step of the reaction is furnished by the observed buffer catalysis.[37] Whereas k_{obsd} is linearly related to acetate and formate concentrations, a saturation phenomena is encountered with phosphate buffer. In the case of Scheme I the parametric values $D = k_3'' \cdot k_1K_a'/(k_{-1} + k_3)$ and $E = k_3''/(k_{-1} + k_3)$; for Scheme II, $D = k_3k_1''/(k_{-1} + k_3)$ and $E = k_{-1}''/(k_{-1} + k_3)$. The ratio of D to E provides an independent check on the other parametric values and equals 6.06×10^5 which compares favorably to a B/C ratio of 4.23×10^5. The saturation phenomenon with phosphate buffer which is not altered by changes in ionic strength or solvent composition (20% v/v dioxane–H_2O) again can be ascribed to a transition from rate-determining ring closure to iminium cation formation with increasing buffer concentration (Scheme I) rather than complexation of buffer and substrate.

A tentative choice between the two schemes can be made on the basis of the Brønsted plot (Figure 8). Buffer data are plotted according to Scheme I, *i.e.*, D/K_a' *vs.* pK_a' with $k_{-1} \gg k_3$, which gives a β value of 0.65. Alternatively the data may be treated in terms of Scheme II which, owing to the relationship of α and β, yields a

(34) K. Koehler, W. Sandstrom, and E. H. Cordes, *J. Am. Chem. Soc.*, **86**, 2413 (1964), and references therein.

(35) The possibility that the steady-state species is **5** can be dismissed on the basis of arguments similar to that given above for the carbinolamine.

(36) W. P. Jencks, *Progr. Phys. Org. Chem.*, 2, 63 (1964).

(37) R. B. Martin, *J. Phys. Chem.*, **68**, 1369 (1964).

Brønsted $\alpha = 0.35$.[38] The low value of α for a general acid catalyzed dehydration of a carbinolamine is not in accord with Brønsted α values observed for general acid catalyzed dehydration of carbinolamines derived from benzylideneaniline,[39] semicarbazone,[40] benzhydrylidenemethylamine,[34] and in 5,10-methylenetetrahydrofolic acid formation.[41] These dehydration reactions are characterized by Brønsted coefficients of 0.7–0.9 and thus are insensitive to the basicity of the amine with catalysis by the solvated proton being predominant. A second difficulty with Scheme II is the requirement of the direct expulsion of hydroxide in the dehydration reaction (k_2). The reverse reaction, hydration of a protonated Schiff base by hydroxide ion attack, is the major pathway for strongly basic amines at alkaline pH[42] but is only found in a limited region of pH for the hydrolyses of Schiff bases of less basic amines. Insofar as the hydrolysis of *p*-chlorobenzylideneaniline is an appropriate model, the pH-independent hydrolysis associated with rate-determining attack of hydroxide ion on the protonated imine occurs in the pH region 9–12.[39] Although it is difficult to predict with absolute certainty the effect of solvent on the magnitude of the Brønsted coefficient, kinetics in the more aqueous media (20% v/v dioxane–H_2O) suggest the continued importance of a pH-independent term in the pH range 6.5–7.5 and a value of $\alpha < 0.5$. On the other hand the large value of the Brønsted coefficient for Scheme I argues that proton transfer from the exocyclic nitrogen to the catalyzing base has occurred to a considerable extent in the transition state.[43] Although it is problematic to deduce conclusions concerned with the degree of formation or cleavage of the pertinent covalent bonds involving the carbon and nitrogen atoms, nevertheless it appears clear in this case that ring formation is probably well advanced. Preequilibrium abstraction of the proton by the base species followed by ring closure in a stepwise process would form the unstable *p*-carboethoxyaniline anion as an intermediate. The preferred mechanism of catalysis generally appears to be that which avoids formation of unstable intermediates and thus a concerted or one-encounter mechanism is preferred.[44]

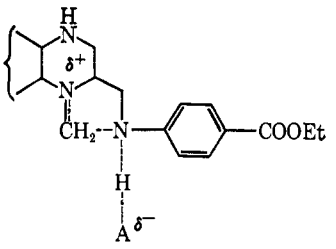

The choice of Scheme I mandates an additional explanation, that is, the magnitude of β. The rates of general base catalyzed hydration of benzhydrylidenedimethylammonium ion by carboxylate anions are correlated with a β of only 0.27;[34] general acid catalysis observed in the dehydration of the carbinolamine intermediate in the oximation of acetone requires a β of 0.4 for the pertinent reverse reaction,[45] and general base catalyzed hydration of ethyl N,N-dimethylthioacetimidate is characterized by a β of 0.6.[46] To the extent that variation in the degree of proton transfer as probed by β reflects the progress along the reaction coordinate for the transition state as a whole, the trend of the above results indicates that the transition state is reached progressively later as the stability of the iminium cation increases with heteroatom substitution[47] which is in accord with the considerations of Hammond[48] and Leffler.[49] That Brønsted slopes are most certainly imperfect probes for the over-all transition-state structure is revealed by the constancy of α for general acid catalysis of attack of semicarbazone on *p*-nitrobenzaldehyde and acetophenone, two substrates which differ in reactivity by two orders of magnitude. It is doubtful that the large value of β in the present case is the result of increased stability of the iminium cation relative to the above examples. Resonance structures which utilize the remaining free *ortho*-amino group are less favorable in terms of the less electronegative atoms involved in charge distribution contrasted to the isoelectronic nitroso group. Moreover, assessed on thermodynamic grounds the presence of a electronegative nitrogen atom in close proximity to a second generally serves to lower the basicity of this nitrogen even though the possibility exists for stabilizing intramolecular hydrogen bonding. This interaction, most likely an ion–dipole repulsion, should act to destabilize to an uncertain extent the iminium cation (**9**). The large value of β may arise from a degree of proton transfer which (1) minimizes the unfavorable free energy change of an uncatalyzed pathway associated with transfer of a formal positive charge from the iminium nitrogen to the nucleophilic nitrogen and the formation of a thermodynamically unstable imidazolidine ring,[50] (2) enhances the low nucleophilicity of the exocyclic amino group, and/or (3) arises from the geometrical requirements for perpendicular approach of the nucleophilic group from an axial position to the pseudoequatorial iminium cation. The latter point is based on the unusually intense ultra-

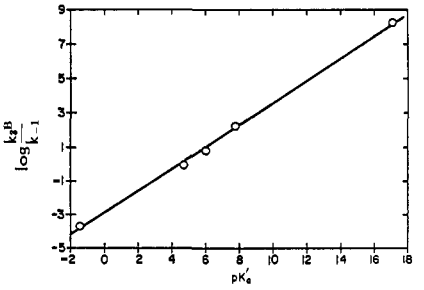

Figure 8. Brønsted plot of the ratio k_3^B/k_{-1} *vs.* pK_a', the latter determined for 50% v/v dioxane–water ($k_3^B = k_3, k_3', k_3''$).

(38) M. Eigen, *Angew. Chem.*, 3, 1 (1964).
(39) E. H. Cordes and W. P. Jencks, *J. Am. Chem. Soc.*, 84, 832 (1962).
(40) E. H. Cordes and W. P. Jencks, *ibid.*, 84, 4319 (1962).
(41) R. G. Kallen and W. P. Jencks, *J. Biol. Chem.*, 241, 5851 (1966).
(42) E. H. Cordes and W. P. Jencks, *J. Am. Chem. Soc.*, 85, 2843 (1963).
(43) L. do Amaral, W. A. Sandstrom, and E. H. Cordes, *ibid.*, 88, 2225 (1966); J. E. Reimann and W. P. Jencks, *ibid.*, 88, 3973 (1966); and G. E. Lienhard and W. P. Jencks, *ibid.*, 88, 3982 (1966). In the present case β for k_{-1} is assumed to be small.
(44) D. R. Robinson and W. P. Jencks, *ibid.*, 89, 7088 (1967).
(45) A. Williams and M. L. Bender, *ibid.*, 88, 2508 (1966).
(46) G. E. Lienhard and T. C. Wang, *ibid.*, 90, 3781 (1968).
(47) R. W. Taft, R. H. Martin, and F. W. Lampe, *ibid.*, 87, 2490 (1965).
(48) G. S. Hammond, *ibid.*, 77, 334 (1955).
(49) J. E. Leffler, *Science*, 117, 340 (1953).
(50) At pH >2.0 there is no experimental evidence for a back reaction or establishment of an equilibrium. At pH <2.0 decomposition of the imidazolidine occurs *via* rearrangement and fragmentation.

violet absorption spectrum of **1** at long wavelengths (310 mμ) which suggests an electronic interaction, perhaps of the charge-transfer type,[51] within a conformation stacking the two aromatic rings. The validity of comparing the β value for hydration to the present case is somewhat tenuous owing to the degree of the solvent effect, although simple polarity considerations predict an increase in β relative to water. Precedent for the general base catalysis required by Scheme I derives from studies on the transimination reaction of benzhydryldimethylammonium cation with methoxyamine and hydroxylamine[34] in which the rate-determining formation of the required *gem*-diamine is subject to catalysis by a second molecule of amine. For reasons not completely understood it is of interest to note that the aminolysis of protonated imido ester is not subject to general catalysis.[52]

In conclusion it is of interest to compare the mechanism for formation of **3** to that for 5,10-methylenetetrahydrofolic acid.[41] The latter reaction exhibits a typical bell-shaped pH–rate profile characteristic of nitrogen derivative formation and interpreted as a result of a change from rate-determining carbinolamine formation on the 5-nitrogen at low pH to rate-determining acid-catalyzed dehydration of carbinolamine at high pH. A number of differences are readily apparent: (1) the K_1 for carbinolamine formation is 32 M^{-1}, *ca.* 150-fold less than found with **1**; (2) the rate of acid-catalyzed dehydration of the carbinolamine of tetrahydrofolic acid is 1.6×10^9 M^{-1} min^{-1} and is therefore 4×10^3 greater than **4** (based on Scheme I); and (3) in the pH region where equilibrium saturation with formaldehyde is obtained the descending leg of the pH profile reflects the dissociation of a proton from the 3-nitrogen amide group incorporated in the pyrimidine ring. The diminished affinity for formaldehyde demonstrated by tetrahydrofolic acid may be the result of a steric repulsion between the hydroxymethyl and the neighboring keto group. The ground-state instability of the carbinolamine in conjunction with increased transition-state stability from a possible lower electron density at the 8-nitrogen because of its greater resonance participation with the heterocyclic ring would act to accelerate acid-catalyzed dehydration relative to **1**. As a result saturation kinetics would be encountered at higher pH values relative to **1**. It is tempting to speculate whether the perturbation in the descending leg of the pH-rate profile caused by ionization of the amide is simply an electronic effect or represents a neighboring group interaction masking the formation of the iminium cation.

In summary the formation of the iminium cation has been demonstrated in the formation of **3** and through arguments based on microscopic reversibility its formation from the imidazolidine through a general acid catalyzed pathway is inferred. This species is an attractive intermediate for the transfer of the methylene unit in Mannich condensations and in the mechanism of action of 5,10-methylenetetrahydrofolic acid.[41,53,54] Its detection at steady-state concentrations depends on a subtle balance between rate constants. If, as suggested, Scheme I is correct, it is necessary that (1) the rate of ring closure, k_3, be less than the rate of hydration, k_{-1}, of the iminium cation and (2) the value of $k_3'K_{wD}$ approximates that of $k_3(H)^+$ within an experimentally accessible pH range. These conditions are subject to electronic effects and therefore testable experimentally. Such reactions in addition to those on the formate level of oxidation are in progress in our laboratory.

(51) L. J. Andrews and R. M. Keefer, "Molecular Complexes in Organic Chemistry," Holden-Day, Inc., San Francisco, Calif., 1964.
(52) E. S. Hand and W. P. Jencks, *J. Am. Chem. Soc.*, **84**, 3505 (1962).
(53) E. C. Wagner, *J. Org. Chem.*, **19**, 1862 (1954).
(54) T. C. Bruice and S. J. Benkovic, "Bioorganic Mechanisms," Vol. II, W. A. Benjamin, Inc., New York, N. Y., 1966.

Experimental Section

The following instruments were used for recording spectra: Varian Model A-60 for nmr, Beckman IR-8 for infrared, Cary 14 for ultraviolet, and A.E.I. MS-9 for mass spectra. All melting points are uncorrected. Analyses were performed by Midwest Microlabs, Indianapolis, Ind.

Materials. The preparation of quinoxaline-2-carboxaldehyde was by the method of Leese and Rydon,[22] mp 107–108° (lit.[22] mp 108°). The desired anils, ethyl N-2′-quinoxalinemethylidene-*p*-aminobenzoate and N-2′-quinoxalinemethylidene-*p*-toluidine, were synthesized as described in published procedures, mp 137–139° (lit.[22] mp 139°) and mp 124–125° (lit.[22] mp 120–121°). Recorded infrared and ultraviolet spectra were consistent with the assigned structures.

Ethyl *p*-[N-2′-(1,2,3,4)-Tetrahydroquinoxalinylmethylene]aminobenzoate. Ethyl N-2′-quinoxalinylmethylidyne-*p*-aminobenzoate (3.27 g, 0.0107 mole) was dissolved in 50 ml of diglyme. To this yellow solution, 1.2 g (0.0295 mole) of sodium borohydride (Metal Hydrides, Inc.) was added as a solid. An additional 25 ml of diglyme was used to rinse any remaining particles of reactant into the flask. The resulting solution was stirred for 1 hr at room temperature. At the completion of the reaction, 12 ml of glacial acetic acid was carefully added, followed by 100 ml of water, after which the solution was made basic by the addition of solid sodium hydroxide pellets. The solution was extracted three times with ether (200 ml); the ethereal layer was washed with 100 ml of water, treated with solid sodium bicarbonate, and dried over anhydrous magnesium sulfate.

The solvent was removed *in vacuo*, yielding 5 ml of brown oil, which solidified when treated with 10 ml of ether; yield of white crystals, 1.43 g (47.5%); mp 131–134°; λ_{max}^{EtOH} 308 mμ (ε 25,400), 221 (31,100); positive to ferric chloride; mass spectrograph parent peak, 310.

The solid material was recrystallized by dissolving it in a minimum amount of hot benzene, followed by the addition of petroleum ether until the solution became cloudy. Cooling the liquid yielded a white, crystalline material: mp 134–135°; λ_{max}^{EtOH} 308 mμ (ε 25,400), 221 (31,100); positive to ferric chloride; infrared absorption at 3350 cm^{-1}. An nmr spectrum in acetone with tetramethylsilane as an internal standard showed a doublet at 7.8 ppm, an unsymmetrical triplet centered at 6.6 ppm, a quartet centered at 4.3 ppm, a complex absorption at *ca.* 3.0–4.0 ppm with a complex multiplet centered at 3.3 ppm, and a triplet at 1.3 ppm with the area ratio 2:6:4:6:3, respectively.

Anal. Calcd for $C_{18}H_{21}N_3O_2$: C, 69.43; H, 6.79; N, 13.49. Found: C, 69.51; H, 7.02; N, 13.47.

N-2′-(1,2,3,4)-Tetrahydroquinoxalinylmethylene-*p*-toluidine. To a stirred solution of N-2′-quinoxalinylmethylidyne-*p*-toluidine (3.579 g, 0.0144 mole) in 65 ml of diglyme was added 1.089 g (0.2787 mole) of sodium borohydride (Metal Hydrides, Inc.). An additional 10 ml of diglyme was used to rinse any remaining particles of reactant into the flask. The resulting solution was stirred for 1 hr at room temperature, during which time a color change from yellow to dark brown was noted.

The resultant solution was acidified by the careful addition of 10 ml of glacial acetic acid, then diluted with 60 ml of water. The solution was then made basic by the addition of solid sodium hydroxide pellets and extracted twice with 75 ml of ether; the ethereal layer was washed with a saturated solution of sodium bicarbonate and dried over anhydrous magnesium sulfate.

The solvent (ether–diglyme) was removed *in vacuo*, yielding a brown oil, which crystallized upon chilling at 0° for 24 hr; yield of white, flocculent crystals, 1.728 g (48.1%).

Recrystallization of the solid material was effected by dissolving it in a minimum amount of hot benzene, followed by the addition of petroleum ether (bp 30–60°) until the solution became cloudy. Cooling the liquid yielded a white, luminescent crystalline material: mp 111–112°; $\lambda_{max}^{100\% EtOH}$ 310 mμ (ε 5100), 252 (15,400), 220

(28,600); positive to ferric chloride; infrared absorption at 3340 cm^{-1}. An nmr spectrum in deuterated chloroform with tetramethylsilane as an internal standard revealed a doublet at 7.0 ppm, a complex multiplet, centered at 6.6 ppm, a singlet at 3.7 ppm, a complex multiplet, centered at 3.2 ppm, and a singlet at 2.2 ppm with the area ratio 2:6:3:5:3, respectively.

Anal. Calcd for $C_{16}H_{19}N_3$: C, 75.85; H, 7.55; N, 16.58. Found: C, 75.63; H, 7.66; N, 16.41.

An alternate procedure for preparation of the above reduced *p*-toluidine derivative based upon the reports of Mosher and DeSelms[23] is as follows. N-2′-Quinoxalinylmethylidyne-*p*-toluidine (1.078 g, 0.0043 mole) was partially dissolved in 50 ml of anhydrous diethyl ether. To this yellow solution, 0.980 g (0.0258 mole) of lithium aluminum hydride (Metal Hydrides, Inc.) in 30 ml of anhydrous ether was added dropwise. An immediate color change from yellow to brown to deep purple was noted. The mixture was stirred under dry nitrogen for 6.5 hr at room temperature. At the completion of the reaction, the excess lithium aluminum hydride was decomposed by the careful addition of 35 ml of a 10% potassium hydroxide solution. The ethereal layer was separated, the aqueous layer was extracted three times with 50-ml portions of ether, and ethereal extracts were combined and dried over magnesium sulfate. The water layer was discarded. The solvent was then removed *in vacuo* to yield a white, crystalline solid with mp 108–109°, with spectral properties identical with the above.

Imidazolidine Adducts. Preparation of 3 and 4. The N-2′-(1,2,3,4-tetrahydroquinoxalinylmethylene) *para*-substituted aniline, 0.30 g (0.0010 mole), was dissolved in 6 ml of purified dioxane to which was added 3 ml of distilled water. A standardized formaldehyde solution (0.07 ml, 0.0011 mole) was added and the solution gently warmed upon a steam bath until a white precipitate appeared. The product was filtered from solution, washed with ether, and recrystallized from benzene–petroleum ether: yield 70%; mp 168–169° (**3**) and mp 195–196° (**4**).

Anal. Calcd for $C_{17}H_{19}N_3$ (**4**): C, 76.97; H, 7.22; N, 15.83. Found: C, 77.54; H, 7.17; N, 15.85.

Anal. Calcd for $C_{19}H_{21}N_3O_2$ (**3**): C, 70.56, H, 6.54; N, 12.98. Found: C, 69.89; H, 6.61; N, 12.93.

The nmr spectrum of **4** in $CDCl_3$ showed aromatic protons centered at τ 3.2 (8 H), the $>NCH_2N<$ AB quartet at 5.37 (J_{ab} = 4 cps), the methylene, methine, and NH protons as a complex multiplet centered at 6.68 (6 H), and the *p*-CH_3 substituent at 7.74.

The nmr spectrum of **3** in dioxane could not be integrated because of limitations imposed by solubility. However, the spectrum clearly showed the $>NCH_2N<$ AB quartet at τ 5.28 (J_{ab} = 5 cps).

The ultraviolet spectra of **3** and **4** are very similar to **2** and **1** in both the position of λ_{max} and the value of ϵ. The value of ϵ 32,900 at $\lambda_{max}^{H_2O}$ 310 for **3** can be assigned with reasonable accuracy on the basis of the observed OD_∞ for the kinetic runs. The infrared spectra of **3** and **4** (Nujol) showed only weak absorption at 3.0 μ.

Kinetics. The instruments employed have been previously described.[55] All reagents were reagent grade. Dioxane used in the kinetic runs was purified by the method of Fieser[56] and freshly distilled from sodium for each day's runs. Water was deionized and double distilled through glass. Under these conditions the above materials were stable for at least 24 hr without further precautions. Formaldehyde solutions were prepared daily from a standard solution of commercial formaldehyde (Fisher), the titer of which was checked routinely.[57]

Kinetic runs were initiated by adding 0.01 ml of a stock dioxane solution of the desired tetrahydroquinoxaline derivative to a cuvette containing 2 ml of the reaction solution, preequilibrated at 25°. The final concentration of tetrahydroquinoxaline was 2–8 $\times 10^{-5}$ *M*. The course of the reaction was monitored by following the formation of product at 310 mμ as a function of time. All experiments were performed at concentrations of formaldehyde in excess over the tetrahydroquinoxaline substrate so that pseudo-first-order kinetics were observed. Plots of log ($OD_\infty - OD_t$) *vs. t* gave as slope/2.303 the value of k_{obsd} (±7%). All OD_∞ values were stable for at least ten half-lives except for solutions at pH <2.5. The observed OD change averaged 0.30 OD units and was pH insensitive. All kinetic runs were in 50% v/v dioxane–water, μ = 0.2 with KCl, 25°, the pH of which was checked before and after the run. The validity of employing glass electrode measurements as an index of hydrogen ion activity in this solvent has been demonstrated by Purlee and Grunwald.[58] The close identity of the predicted pH for solutions of known buffer composition and that measured by the glass electrode was confirmed in the course of the kinetic experiments. No changes in rate were found on changing μ to 0.3. All kinetic runs exhibited to a varying degree (concentration of formaldehyde and pH dependent) an initial lag phase indicative of preequilibrium carbinolamine formation. The pK_a' values of **1**, **7**, and **3** were measured potentiometrically and spectrophotometrically in accordance with procedures described in ref 30.

Acknowledgment. This work was supported by Research Grant GB-7246 from the National Science Foundation.

(55) S. J. Benkovic and P, A. Benkovic, *J. Am. Chem. Soc.*, **88**, 5504 (1966),

(56) L. F, Fieser, "Experiments in Organic Chemistry," 3rd ed, D. C. Heath, Inc., Boston, Mass., 1955, p 284.

(57) J. F. Walker, "Formaldehyde," American Chemical Society Monograph Series, Reinhold Publishing Corp., New York, N. Y,, 1964.

(58) E. L. Purlee and E. Grunwald, *J. Am, Chem. Soc.*, **79**, 1366 (1957).